Available online at www.sciencedirect.com
SCIENCE DIRECT®
Thermochimica Acta 404 (2003) 71–79
thermochimica acta
www.elsevier.com/locate/tca

The influence of ultrasound on the thermal behaviour of a well ordered kaolinite

F. Franco [a,*], L.A. Pérez-Maqueda [b], J.L. Pérez-Rodríguez [b]

[a] *Departamento de Química Inorgánica, Cristalografía y Mineralogía, Facultad de Ciencias, Campus de Teatinos, Universidad de Málaga, 29071 Málaga, Spain*
[b] *Instituto de Ciencia de Materiales de Sevilla, Centro Mixto CSIC, Universidad de Sevilla, C/Américo Vespucio s/n, Isla de la Cartuja, 41092 Sevilla, Spain*

Received 12 August 2002; received in revised form 22 January 2003; accepted 24 January 2003

Abstract

The present study examines the effect of sonication on the structure and on the thermal behaviour of a well ordered kaolinite. XRD data indicated that sonication produces an increase of the translation disorder of kaolinite layers as well as delamination and particle-size reduction along the *b*-axis. As a consequence of this particle-size reduction the surface area increases sharply with sonication time from 8.5 to 83 m^2/g, after 20 h of treatment. When sonication time increases, the original dehydroxylation effect shifts to lower temperatures, is narrowing and decreases in intensity at the same time that the exothermic effect, previous to the mullite formation shifts to lower temperatures and notably broadened.

Keywords: Kaolinite; Sonication; Thermal behaviour; Translation defects

1. Introduction

Kaolinite has been and continues to be one of the most important and useful industrial minerals. Kaolinite has important applications, e.g. as a coating and filler in the manufacturing of paper, as extender in inks and paints, as starting material for aluminosilicate-based ceramics, as cracking catalysts, as raw material in the production of fibreglass, as additive in the production of rubber and polymers, etc.

The physical and chemical properties of kaolinite determine its use as an industrial mineral. Some applications of kaolinite are closely related to its surface reactivity. This surface reactivity can be enhanced with a particle-size reduction which, traditionally, has been produced by grinding (either wet or dry).

Grinding of kaolinite has been the subject of research for a long time [1–6]. Shaw [1] studied the effect of grinding on kaolinite clay colloids using electron microscopy. This author indicated that wet grinding caused shearing along the cleavage planes whereas dry grinding fractured the crystal. Sánchez-Soto et al. [7] pointed out that grinding of kaolinite produced strong structural alterations along the *c*-axis resulting in disorder and total degradation of the crystal structure of kaolinite and the formation of an amorphous product. They observed that surface area increased with grinding time as a result associated with particle-size reduction. However, the particles of kaolinite became more agglomerated with grinding, and the surface area decreased after 30 min. There was a limit to particle-size reduction with grinding [7].

* Corresponding author. Fax: +34-952-132-000.
E-mail address: ffranco@uma.es (F. Franco).

0040-6031/$ – see front matter © 2003 Elsevier Science B.V. All rights reserved.
doi:10.1016/S0040-6031(03)00065-0

On the other hand, dehydroxylation of kaolinite is also affected by grinding. The endothermic effect related with the dehydroxylation process shifted to lower temperatures (from 565 to 490 °C) after 180 min of treatment, and disappeared completely above this time [7].

Kristóf et al. [8] discussed the amorphisation of kaolin in a planetary mill. They observed that 1 h of amorphisation is necessary to produce mullite type crystal at 1000 °C.

A feasible technique for particle-size reduction is ultrasound. The extended application of ultrasound as a tool for material chemistry began only in 1980. Cavitational collapse sonication on solids leads to microjet and shock-wave impacts on the surface, together with interparticle collision, which can result in particle-size reduction [9]. Pérez-Maqueda et al. [10] shown that sonication of macroscopic vermiculite flakes yields submicron plate-like particles and that even after 100 h sonication time, vermiculite was not amorphisized and the crystalline structure was not damaged.

In the present study, the effect of ultrasound in the structure and thermal behaviour of a well ordered kaolinite is extensively studied. Changes in specific surface area, crystallite size, crystallinity indices and dehydroxylation processes have been analysed.

2. Experimental

2.1. Material

The starting material used for this study (KGa-1) is a well ordered kaolinite from Washington County, Georgia, with a Hinckley index (HI) of 1.19 [11]. This kaolinite powder has been previously characterised [7,12].

2.2. Preparation of treated samples

Ultrasonic treatment was performed with a Misonic ultrasonic liquid processor of 750 W output with a 20 kHz converter and tapped titanium disrupter horn of 12.7 mm in diameter that produce a double (peak to peak) amplitude of the radiating face of the tip of 120 μm. The horn tip was dipped into a cylindrical jacketed cooling cell of 5 cm in internal diameter, where 1.5 g of kaolinite were mixed with 40 ml of freshly deionised water. The dispersions were sonicated for periods ranging from 5 to 20 h. The temperature reactor was kept constant at 20 °C during the entire treatment by means of a cooling recirculator. After treatment, samples were lyophilised to remove the water of the suspension.

2.3. Sample characterisation

Brunauer–Emmet–Teller (BET) specific surface areas were obtained with an automatic system (model No. 2200 A, Micromeritics Instrument Corp., Norcross, GA), using nitrogen gas as an adsorbate at liquid nitrogen temperature. The samples previously were outgassed at 140 °C for 2 h.

X-ray diffraction (XRD) patterns were obtained using a Siemens D-5000 diffractometer. The XRD patterns were obtained using Cu Kα radiation, at 40 kV and 35 mA, and a step size of 0.02° 2θ at a counting time of 3 s. Measurements were performed on randomly oriented powder preparations. Defects in kaolinite were characterised using the HI [11] and the R_2 index of Liètard and others [13,14]. The HI value was calculated as the ratio of sum of the height above background of the (1 1 0) and (1 1 $\bar{1}$) reflections against the band of overlapping reflections occurring between 20 and 23° 2θ compared to the total height of the (1 $\bar{1}$ 0) above background. R_2 was calculated with the (1 $\bar{3}$ 1) and (1 3 1) reflections intensities and the counts in the valley between them. The apparent coherent scattering thickness of the kaolinite crystals was calculated along the c^*-axis, using the (0 0 2) reflection (CS_{002}), and along the *b*-axis using the (0 6 0) reflection (CS_{060}), according to the Scherrer formula [15].

The untreated kaolinite and the sonicated samples were spread on a platinum (Pt) holder of a Siemens D-5000 diffractometer. The high temperature X-ray diffraction (HTXRD) patterns were obtained using Cu Kα radiation at 40 kV and 30 mA, a step size of 0.02° 2θ and a counting time of 1 s. Heating rate was 4 K/s. The samples heated to a particular temperature were held at that temperature for 600 s prior to the XRD pattern being acquired. Diffractograms were obtained after variable temperature intervals (between 50 and 100 °C) according to the expected modifications indicated by the DTA–TG curves.

TG and DTA measurements of the untreated kaolinite and sonicated samples were done in a simultaneous

TG–DTA instrument (Thermoflex, Rigaku Co. Ltd., Tokyo, Japan). The instrument temperature was calibrated with indium and aluminium. Alumina was used as reference for DTA measurements. An amount of sample in the range between 40 and 45 mg was loosely packed into a platinum crucible. Experiments were performed in static air at a heating rate of 10 K/min.

3. Results

3.1. Specific surface area measurements

Fig. 1 shows the variation of the specific surface area for the KGa-1 sample as a function of sonication time. The plot clearly shows that sonication produces a remarkable increase in the specific surface area with a treatment time between 0 and 20 h. The specific surface area of kaolinite samples increased from 8.5 to 35.2 m^2/g after 10 h of treatment, as shown in Fig. 1. This surface area variation is associated with particle-size reduction. The specific surface area continued increasing with the sonication time reaching 83 m^2/g after 20 h (Fig. 1). This result is very interesting because it shows that increments in the specific surface area obtained with ultrasound energy are notably higher than those obtained with a simple grinding. Previous studies have determined that when this kaolinite was ground in a ball mill the maximum increase in specific surface area (from 8.5 to 18.31 m^2/g) was obtained after 15 min of treatment [7]. Above this time the particles become more agglomerated, and the surface area decreases as a consequence of the enhanced surface energy of the ground particles [7,16,17]. However, when the increase in specific surface area is enhanced with ultrasound treatment this increase continues exponentially with time of treatment reaching specific surface areas never obtained with this kaolinite. Possibly, the high agitation to which are subjected the particles of kaolinite in the ultrasound treatment causes its desegregation, preventing thus the agglomeration of the particles of kaolinite.

4. X-ray diffraction analyses

Fig. 2 shows the XRD patterns of the untreated kaolinite and the sonicated samples at increasing times of treatment, between 20 and 40° 2θ. The reflection (0 2 l), (1 1 l) and (2 0 l), (1 3 l) of the untreated

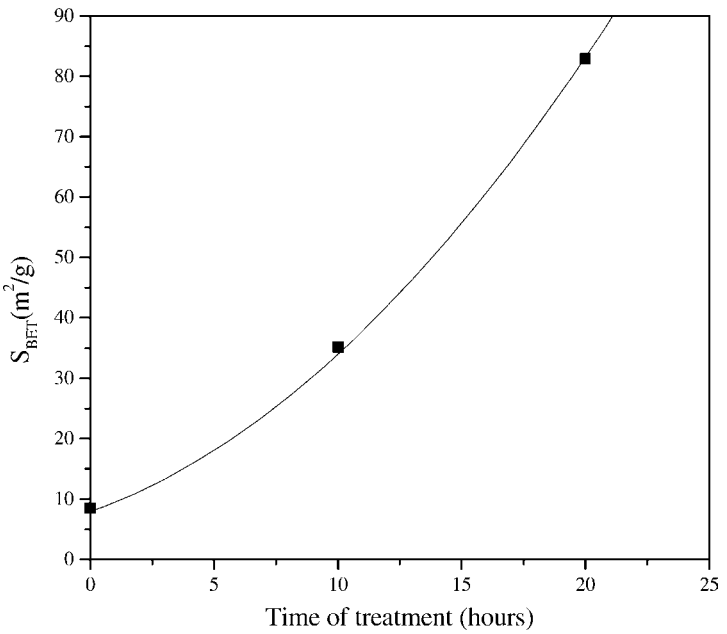

Fig. 1. Specific surface area vs. time of treatment.

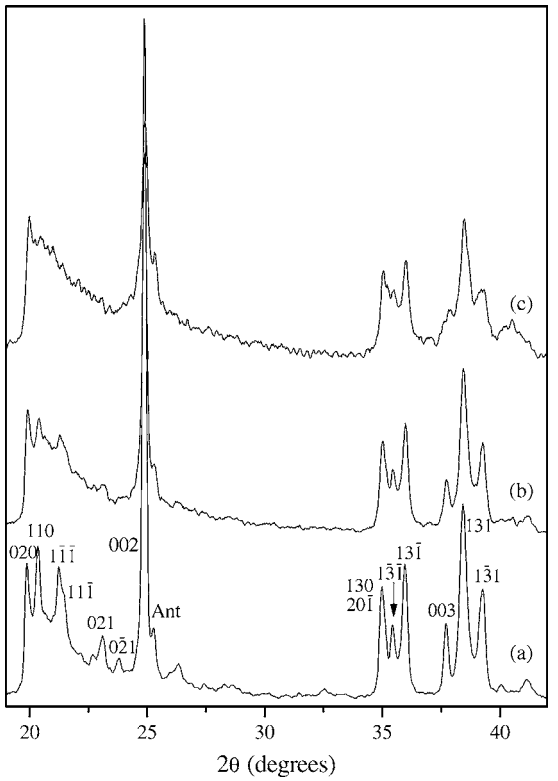

Fig. 2. XRD patterns of the untreated kaolinite (a); the 10 h sonicated kaolinite (b); and the 20 h sonicated kaolinite (c); obtained from randomly oriented powder preparations.

kaolinite (Fig. 2a) are narrow and intense, indicating that this kaolinite is a well ordered specimen. However, Plançon and Tchoubar [18], in a previous study, have shown that this sample contains stacking faults that consist of the presence of a small proportion of random shifts of layers and faults by displacement of the Al vacancies.

Comparisons of the diffraction peak profiles of the sonicated samples with those of the untreated kaolinite shows that the ultrasound treatment produced.

1. A broadening of the (0 0 2) reflection, which indicates that the thickness of the kaolinite crystallite decreased with treatment. The apparent coherent scattering thickness of kaolinite particles along the *c*-axis decreases from 424 to 368 Å after 10 h of treatment and to 270 Å after 20 h of ultrasound treatment (Table 1). Thus, the number of layers within an individual crystallite decreases from 59 to 51 Å after 10 h, and to 38 Å after 20 h of ultrasound treatment.
2. A progressive broadening of the (0 6 0) reflection, which indicates that the dimension of kaolinite crystals along their *b*-axis also decreases with the time of ultrasound treatment. The apparent coherent scattering thickness of kaolinite particles along the *b*-axis decreases from 261 to 231 Å after 10 h of treatment and to 202 Å after 20 h of ultrasound treatment.
3. An important modification of the (0 2 *l*), (1 1 *l*) reflections. These reflections are very sensitive to the abundance of translation defects consisting of random and specific interlayer displacement of type $-a/3+b/3$ [19]. We have used the HI [11] to evaluate the modifications in this zone of diagrams (20–22° 2θ) and for assigning a numerical value for the degree of structural disorder (Table 1). The decrease of the HI from 1.19 to 0.33 indicates that a great increase in translation defects takes place at 10 h of treatment whereas above this time a minor decrease of the HI indicates a lower increasing in translation defects, between 10 and 20 h of treatment (0.33–0.21).
4. Minor modifications on the (2 0 *l*) and (1 3 *l*) reflections. For this reason the possibility of $\pm 2\pi/3$ rotations among the adjacent layers in particles must be discarded [18]. This zone of diagrams (35–40° 2θ) is also affected by random displacements [14]. Increasing the small displacements (random displacements) between adjacent layers is the principle effect of reducing the (1 3 1) reflection relative to the (1 $\bar{3}$ 1) reflection [19]. We have used the R_2 parameters [13] to measure the

Table 1
Treatment conditions and crystalline data of the starting kaolinite and of sonicated kaolinites

Sample	*T* (h)	HI	R_2	*D* ((1 3 1) to (1 $\bar{3}$ 1))	CS_{002}	CS_{060}
KGa-1[a]	0	1.19	0.99	0.86	424	261
	10	0.33	0.88	0.84	368	231
	20	0.21	0.71	0.72	270	202

T: time of treatment in hours; HI: Hinckley index [11]; R_2: index of Lièrtard and others [13,14]; *D*: distance between (1 3 1) and (1 $\bar{3}$ 1) in 2θ (°); CS_{002} and CS_{060}: apparent coherent scattering thickness measured using the Scherrer formula on (0 0 2) and (0 6 0) reflections.

[a] Starting kaolinite (K, kaolinite).

modifications in this zone of the diffractograms. The R_2 parameter decreases from 0.99 to 0.88 at 10 h and to 0.71 at 20 h of treatment.

5. A slight narrowing between (1 3 1) and (1 $\bar{3}$ 1) reflections, which is related with a minor difference between γ and 90°. This narrowing indicates the formation of layers having vacant octahedral C-sites (dickite-like layers) [19]. The distance of these reflections (2θ (°)) are reported in Table 1. The distance between (1 3 1) and (1 $\bar{3}$ 1) reflections decreases slightly from 0.86 to 0.84° 2θ in the first 10 h of treatment whereas between 10 and 20 h of treatment the narrowing between this reflections is higher and the distance decreases from 0.84 to 0.72° 2θ at 20 h.

4.1. Thermal analysis

The DTA–TG curves of the untreated kaolinite and the sonicated samples are shown in Fig. 3a. The TG curve of untreated kaolinite (Fig. 3a) shows that its heating at a continuous rate originates a slight mass loss below 150 °C, associated with the loss of the loosely adsorbed water on the particle surface. Between 150 and 300 °C the TG curve shows that the mass remains constant, whereas a slight mass loss between 300 and 440 °C followed by higher mass loss from 440 to 800 °C, associated with the dehydroxylation process, occurs. The DTA curve (Fig. 4a) shows that the dehydroxylation process originates an endothermic effect (between 398 and 672 °C) centred at 542 °C. At higher temperature, an intense exothermic effect is also observed (between 961 and 1004 °C) at 987 °C, which is related with the formation of either mullite nuclei or a phase with a spinel-type structure, an γ-alumina or cubic phase or both [20,21].

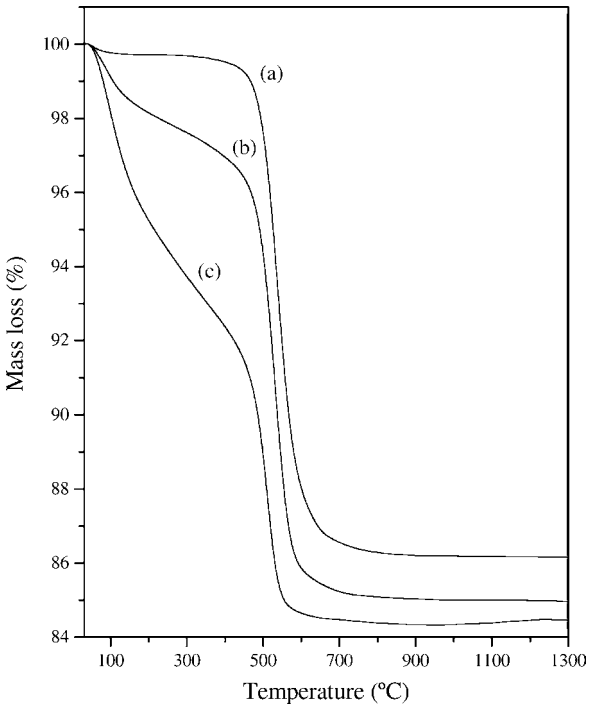

Fig. 3. TG curves of the untreated kaolinite (a); 10 h sonicated kaolinite (b); and 20 h sonicated kaolinite (c).

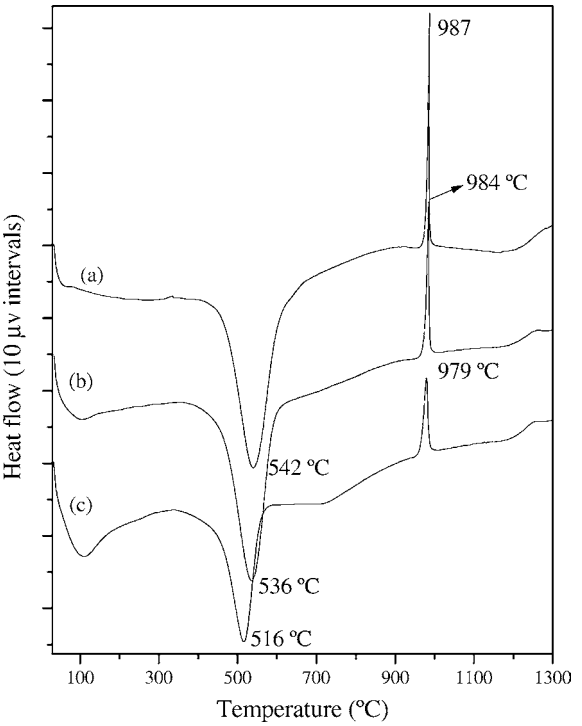

Fig. 4. DTA curves of the untreated kaolinite (a); 10 h sonicated kaolinite (b); and 20 h sonicated kaolinite (c).

The TG curve of the kaolinite sonicated during 10 h (Fig. 3b) shows a greater mass loss below 150 °C compared to that observed in the TG curve of untreated kaolinite. From this temperature, contrary to that observed in the untreated kaolinite, the mass continues decreasing. From 420 °C, a change in slope on the TG curve leads to a higher mass loss. The mass loss

stops at 800 °C indicating the end of the dehydroxylation process. The DTA curve of this sample (Fig. 4b) shows an endothermic effect centred at 100 °C associated to the loss of the adsorbed water. The endothermic effect due to dehydroxylation of kaolinite appears shifted to lower temperatures (from 542 to 536 °C after 10 h of sonication). This later endothermic effect (between 360 and 633 °C) is slightly narrower than that observed in the DTA curve of untreated kaolinite, the FWHM of this peak decreases from 89 to 77 °C in 10 h of treatment. This narrowing can be related with an homogenisation of the particle size of kaolinite. Thus, the DTA curve also shows that the position and the width of the exothermic effect appears slightly affected by the first 10 h of sonication treatment (Fig. 4b).

The thermoanalytical curves of the kaolinite sonicated during 20 h show that the thermal processes involved in the continuous heating rate of kaolinite are notably affected after this sonication time (Figs. 3c and 4c). Firstly, the mass loss below 150 °C is notably higher to the observed in the untreated kaolinite and in the kaolinite sonicated during 10 h. This increase in the mass loss below 150 °C is accompanied by an increase in the area of the endothermic effect centred at 100 °C (Fig. 4c) and is related with an increase of the amount of the adsorbed water, due to the increase in the specific surface area. From 150 to 420 °C, the TG curve shows a greater mass loss compared to that observed in the TG curve of untreated kaolinite and in the kaolinite sonicated during 10 h. Nevertheless, this mass loss is not accompanied by a defined endothermic effect (Fig. 4c). From 420 °C, in a similar way to that observed in the TG curve of the kaolinite sonicated during 10 h, a change in slope on the TG curve leads to a higher mass loss, which correspond to the dehydroxylation of kaolinite. The DTA curve of this sample indicates that this dehydroxylation process is notably affected by the ultrasound treatment. The endothermic effect related with this process (Fig. 4c) shifted from 542 to 516 °C after 20 h of treatment. The width of this endothermic peak also decreased with time of treatment (FWHM decreases from 89 to 63 °C) indicating that the application of the ultrasound energy leads to an homogenisation of the dehydroxylation process. Both the temperature and width of the exothermic effect also appears strongly influenced by sonication. This exothermic peak, observed between

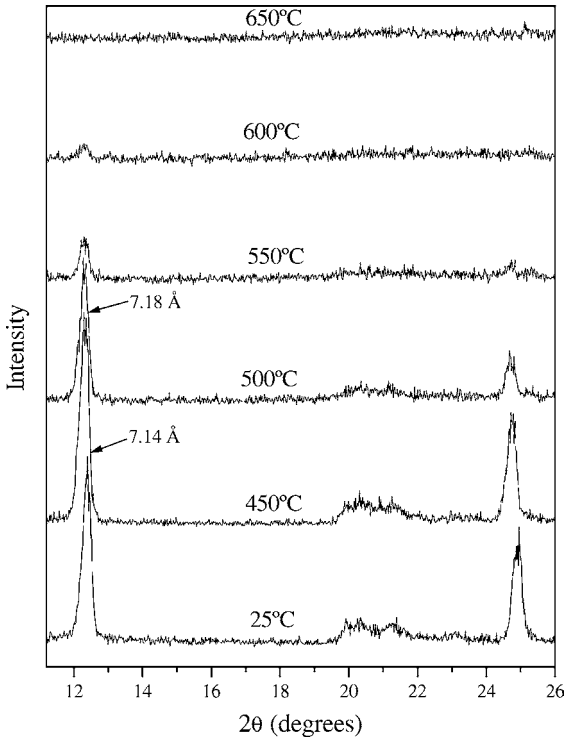

Fig. 5. Selected HTXRD patterns of the untreated kaolinite obtained after heating in the range 25–650 °C.

953 and 996 °C, shifted from 987 to 979 °C and notably broadened after 20 h of sonication (the FWHM of this exothermic peak increases from 3.5 °C in untreated kaolinite to 11.37 °C after 20 h of treatment).

4.2. HTXRD results

The HTXRD patterns of the untreated kaolinite obtained at increasing temperatures are shown in Fig. 5, and the intensities of the first basal reflection of the untreated kaolinite and sonicated samples during 10 and 20 h versus temperature are plotted in Fig. 6. The HTXRD patterns permitted the distinction of the processes occurred in the room temperature to 750 °C interval. In the case of the untreated kaolinite, in a first stage the heating from room temperature to 450 °C originates a slight increase in the intensity of the (0 0 1) reflections (Figs. 5 and 6) due to the loss of adsorbed molecules, which probably lead to a better order in the packing of the kaolinite [22]. However, a slight dilation of the structure perpendicularly to the layers

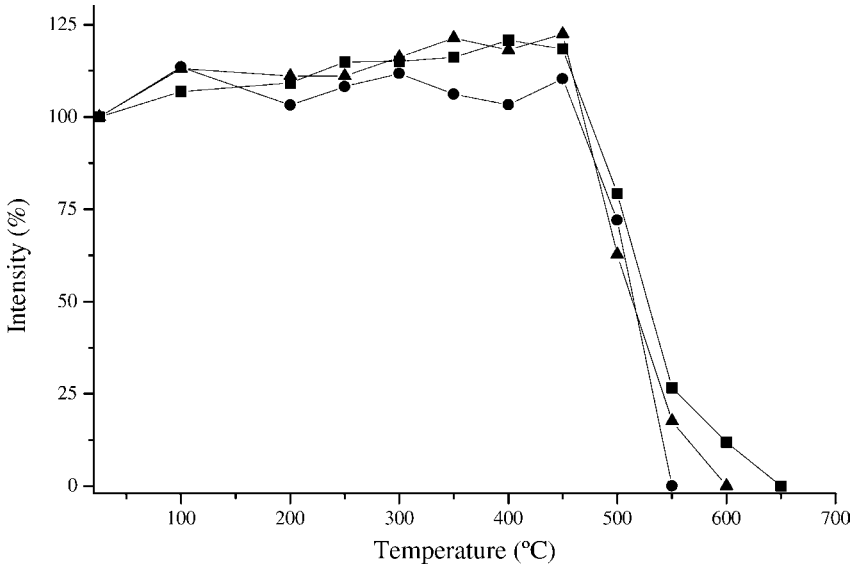

Fig. 6. Variation of the intensity of the basal reflection of the untreated kaolinite (full square), 10 h sonicated kaolinite (full triangle) and 20 h sonicated kaolinite (full circle) in the temperature range of 25–650 °C.

(from 7.14 to 7.18 Å) is observed at 450 °C. In a second stage, the decrease in intensity of the kaolinite reflection above 450 °C indicates the beginning of the dehydroxylation process. This is also in accordance with the DTA–TG results (Figs. 3 and 4), which reveal that the endothermic effect due to dehydroxylation process begins at ca. ∼450 °C. The HTXRD patterns shows that the kaolinite (0 0 1) reflection remains until 600 °C showing, at this temperature, 12% of its initial value. At 650 °C the (0 0 1) reflection disappeared completely indicating thus the end of the dehydroxylation process.

The HTXRD patterns of the sonicated sample during 10 h shows a similar behaviour to that observed in the HTXRD pattern of untreated kaolinite. In a similar form, in the range between room temperature and 450 °C, the (0 0 1) reflection increases slightly (Fig. 6), showing, also, a dilation of the structure along *c*-axis from 7.14 to 7.16 Å in this temperature range. From 450 °C this reflection decreases slightly stronger than the (0 0 1) reflection of untreated kaolinite and remains until 550 °C showing, at this temperature, 17% of its initial value. At 600 °C the (0 0 1) reflection disappeared indicating that the end of the dehydroxylation process occurred at lower temperatures to that observed in the HTXRD of the untreated kaolinite.

The HTXRD patterns of the sonicated kaolinite during 20 h show in the first stage, between room temperature and 450 °C, a minor dilation of the structure along the *c*-axis (from 7.14 to 7.15 Å) compared to that observed in the HTXRD patterns of the untreated and 10 h treated kaolinite. From 450 °C (Fig. 6) the dehydroxylation process causes the decreases of the (0 0 1) reflection of kaolinite which disappears completely at 550 °C.

5. Discussion

The specific surface area analysis, the X-ray patterns, the DTA–TG curves and the HTXRD patterns showed that the structure and the thermal behaviour of kaolinite were strongly affected by the ultrasound treatment.

The first and more evident change produced by this treatment is the great increase in specific surface area obtained. Sánchez-Soto et al. [7], in a previous work, shown that dry grinding in a ball mill of this kaolinite caused an increase in the specific surface area from 10.20 to 18 m^2/g after 15 min of treatment. Above this time the particles become more agglomerated, and the specific surface area began to decrease, as a

consequence of the enhanced surface energy of the ground particles, caused by the grinding. Similar behaviours were found previously after grinding of other kaolinites by several authors [8,23]. Contrarily to that observed in the grinding studies, when the increase in specific surface area is obtained from an ultrasound treatment, this is exponential and no decrease is observed even after 20 h of treatment. Apparently, the strong agitation to which the particles are subjected is greater than the surface energy created with the impacts and it prevents the formation of agglomerated particles.

The XRD patterns of the treated samples indicate that the structural changes induced by the ultrasound treatment are time depended. After 10 h of treatment, the ultrasound energy caused a great increase of the abundance of translation defects consisting of displacement of type $-a/3 + b/3$ and random translations, as shown the great decrease of the HI. In addition, a decrease of the thickness of the kaolinite plates and a minor decrease of the dimensions of the particles along their *b*-axis are also observed. After 20 h of treatment, the ultrasound energy caused a minor decrease in the HI but caused a greater decreasing of the R_2 index, which indicates an increase in random translation. In this case, a larger delamination effect, is observed together with a greater decrease of the CS_{002} parameter. Nevertheless, the variation in the CS_{060} shows a similar cross breakage of the kaolinite particles compared to that obtained in the first 10 h of treatment. However, in spite of the formation of translation defects, the structure of kaolinite still remains, contrarily to that observed in the grinding treatments, where a total degradation of the kaolinite structure, probably related to the rupture of the octahedral and tetrahedral layers, occurred after 2 h of grinding [7].

The TG curves indicated that ultrasound treatment also produced an increase in mass loss on heating at $<420\,^{\circ}C$, in accordance with grinding treatment. Nevertheless, the HTXRD patterns of the ultrasound treated kaolinite showed no decrease of the (0 0 1) reflection of kaolinite in this temperature range. This result suggests that this mass loss correspond to the loss of some ions formed during the ultrasound treatment and weakly bonded hydroxyl groups of the kaolinite layers, possibly located on the new generated surface, which evolved within this temperature range with no destruction of the 7 Å structure. Similarly to that observed by González García et al. [24] in the grinding of kaolinite, the ultrasound treatment causes a loss of OH ions and the formation of other ions which are removed at low or medium temperatures.

The DTA curves indicated that the endothermic effect corresponding to dehydroxylation process shifts to lower temperatures and decreases in area, as ultrasound treatment time increases. The HTXRD patterns shown that the end of dehydroxylation process is shifted to lower temperatures with the ultrasound treatment. Possibly, this shift is caused by the particle-size reduction and the structural disorder induced by the sonication treatment.

The exothermic peak at $987\,^{\circ}C$ is also affected by the ultrasound treatment, this peak shift to lower temperatures and is notably broadened as ultrasound treatment time increases. According to Kristóf et al. [8], this decrease in temperature may be attributed to the deformation of Si–O–Al bonds produced by mechanical forces.

6. Conclusions

Sonication produces not only an important delamination effect on the kaolinite sample but also a reduction of the other particle-dimension and an increase in the amount of translation defects. As a consequence of these effects, the surface area increases exponentially. These structural modifications also influence strongly the thermal behaviour of the sonicated kaolinite. When sonication time increases, the mass loss below $420\,^{\circ}C$ considerably increases; the endothermic effects corresponding to dehydroxylation of kaolinite shifts to lower temperatures, is narrower and decreases in intensity as the sonication time increases; at the same time that the exothermic effect previous to the mullite formation shifts to lower temperatures and is notably broadened.

References

[1] B.T. Shaw, J. Phys. Chem. 46 (1942) 1032.
[2] W.D. Laws, J.B. Page, Soil Sci. 62 (1945) 319.
[3] R.D. Dragsdorf, H.E. Kissinger, A.T. Perkins, Soil Sci. Soc. Am. 71 (1951) 439.
[4] T. Haase, K. Winter, Bull. Soc. Fr. Ceram. 44 (1959) 13.
[5] J.G. Miller, T.D. Oulton, Clays Clay Miner. 18 (1970) 313.

[6] Z. Juhasz, Acta Miner.-Petrogr. 24 (Suppl.) (1980) 121.
[7] P.J. Sánchez-Soto, M.C. Jiménez de Haro, L.A. Pérez-Maqueda, I. Varona, J.L. Pérez-Rodríguez, J. Am. Ceram. Soc. 83 (2000) 1649.
[8] E. Kristóf, A.Z. Juhász, I. Vassányi, Clays Clay Miner. 42 (1993) 608.
[9] D. Peters, J. Mater. Chem. 6 (1996) 1605.
[10] L.A. Pérez-Maqueda, O.B. Caneo, J. Poyato, J.L. Pérez-Rodríguez, Phys. Chem. Miner. 28 (2001) 61.
[11] D.N. Hinckley, Clays Clay Miner. 11 (1963) 229.
[12] H. Van Olphen, J.J. Fripiat, Data Handbook for Clay Minerals and Other Non-Metallic Minerals, Pergamon Press, Oxford, 1979, p. 346.
[13] O. Lièтard, Ph.D. thesis, Nancy, France, p. 345.
[14] J.M. Cases, O. Lièтard, J. Yvon, J.F. Delon, Bull. Miner. 105 (1982) 439.
[15] B.D. Cullity, Elements of X-ray Diffraction, Addison-Wesley, Reading, MA, 1956, p. 514.
[16] J. Cornejo, M.C. Hermosín, Clay Miner. 23 (1988) 391.
[17] J.L. Pérez-Rodríguez, P.J. Sánchez-Soto, J. Therm. Anal. 37 (1991) 1401.
[18] A. Plançon, C. Tchoubar, Clays Clay Miner. 25 (1977) 436.
[19] A. Plaçon, C. Zacharie, Clay Miner. 25 (1990) 249.
[20] K. Okada, N. Otsuka, J. Ossaka, J. Am. Ceram. Soc. 69 (1986) 51.
[21] B. Sonuparlak, M. Sarikaya, I.A. Aksay, J. Am. Ceram. Soc. 70 (11) (1987) 837.
[22] F. Franco, M.D. Ruiz Cruz, Clays Clay Miner. 50 (2002) 46.
[23] G. Suraj, C.S.P. Iyer, S. Rugmini, M. Lalithambika, Appl. Clay Sci. 12 (1997) 111.
[24] F. González García, M.T. Ruiz Abrio, M. González Rodríguez, Clay Miner. 26 (1991) 549.